

Exact ground states for the four electron problem in a Hubbard ladder.

Endre Kovács and Zsolt Gulácsi

Department of Theoretical Physics, University of Debrecen, H-4010 Debrecen, Hungary

(Dated: February 10, 2018)

Abstract

The exact ground state of four electrons in an arbitrary large two leg Hubbard ladder is deduced from nine analytic and explicit linear equations. The used procedure is described, and the properties of the ground state are analyzed. The method is based on the construction in \mathbf{r} -space of the different type of orthogonal basis wave vectors which span the subspace of the Hilbert space containing the ground state. In order to do this, we start from the possible microconfigurations of the four particles within the system. These microconfigurations are then rotated, translated and spin-reversed in order to build up the basis vectors of the problem. A closed system of nine analytic linear equations is obtained whose secular equation, by its minimum energy solution, provides the ground state energy and the ground state wave function of the model.

PACS numbers:

I. INTRODUCTION

Often, several authors have underlined that in understanding strong correlation effects presumably new methods of attack and new languages are necessary (Senthil 2004). Starting on this line, in the case of finite value of the concentration of carriers in the studied materials, several non-perturbative procedures have been recently worked out, of which we mention the following ones. 1) Bozonization techniques (Tomonaga 1950) reactualized in mid-1990s (Gulácsi 1997, Shankar 1994) and even extended to finite temperatures (Bowen and Gulácsi 2001), have been applied for several systems as Coulomb blockade in quantum dots (Golden and Halperin 2002), mesoscopic wires (Torres 2002), two-band cases (Gulácsi and Anderson 1998), ferromagnetism (Honner and Gulácsi 1977, 1997, 1998, 1999), density waves (Orignac and Citro 2003), or metal-insulator transitions (Gulácsi and Bedell 1994). The procedure has been also used in the study of different model characteristics for example, in the case of t-J (Chen and Wu 2002), Luther-Emery (Orignac and Poiblan 2003), or Kondo (McCulloch and Gulácsi 2002, McCulloch et al. 2001,2002) models. 2) Infinite order canonical transformations applied for the Anderson and multiband Hubbard models (Chan and Gulácsi 2001, Gulácsi and Anderson 1998), and 3) Decomposition of the Hamiltonian in positive semidefinite operators, leading to interesting new phases (Gulácsi 2004a), also in three dimensions (Gulácsi and Vollhardt 2003), or even disordered and interacting (Gulácsi 2004b) cases.

In the last years, several experimental results have directed the attention to experimental situations suggesting interesting technological application possibilities, where the strong correlation effects emerge not at finite concentration value of electrons, but for few electrons confined in a system or device. Such situations related to condensed matter physics, are encountered on a large spectrum of subfields, as for example in the case of quantum dots (Maksym et al. 2000), quantum wells (Kochereshko et al. 2003), mesoscopics (Halfpap 2001), entanglement (Sackett et al. 2000), etc. This subject attracted increasing interest from the point of view of the theoretical description in the last decade. Starting from even one electron problems solved exactly (Sigrist et al. 1991), several cases of interest for two (Kovács and Gulácsi 2001), three (A. Amaya-Tapia et al. 2004, Davydychev and Delbourgo 2004), four (Zhang and Henley 2004), or few (Papadopoulos 2001, Zhou et al. 2002) particles have been studied. Concretely, in the case of $N_p = 4$ particles, even if the simulation

have been started more than a decade ago (Traynor et al. 1991, Uesaka et al. 1993), only few valuable results are known in this subject in the condensed matter context, as for example the energy dependence of the maximal Lyapunov exponent for 1D Lenard-Jones system (Okabe et al. 2004), the behaviour of a simplified spinless fermion correlated electrons model (Zhang and Henley 2004), or doped quantum well structures (Kochereshko et al. 2003). As can be seen, the collected information, at least at the moment, provides only a poor characterization of the experimental situations of interest.

In this paper, extending the frame of the non-perturbative methods mentioned above to the case of the low density limit, and starting from the aim to provide valuable high quality essential information for the $N_p = 4$ case, we provide exact results for this field, presenting the exact ground state for four interacting electrons in an arbitrary large two leg Hubbard ladder, characterized by periodic boundary conditions. For this to be possible, a direct \mathbf{r} -space representation is used for the wave functions. On this line first symmetry adapted ortho-normalized basis wave vectors are constructed starting from local particle configurations. Based on these, an explicit and analytic closed system of equations is provided for nine type of basis wave vector components, whose secular equation leads to the ground state wave function and the ground state energy of the system.

Deducing the ground state wave function for different microscopic parameters of the model, ground state expectation values are calculated for different physical quantities of interest, and correlation functions are deduced in order to characterize the ground state properties.

For the case of the low density limit, the procedure presented here, enrolls under the requirement of new languages. Comparing the deduced ground states to ground states obtained in similar conditions for square systems (Kovács and Gulácsi 2004) at exact level, the emerging differences suggest that is highly questionable to approach at a good quality level, the two dimensional behaviour from the ladder side.

The remaining part of the paper is structured as follows. Section II. presents the Hamiltonian, Section III. describes the used procedure, Section IV. characterizes the deduced ground states, and Section V. containing the summary and conclusions closes the presentation.

II. THE HAMILTONIAN

The Hamiltonian of the Hubbard ladder is used in a standard form

$$\hat{H} = t\hat{t} + U\hat{U}, \quad (1)$$

where

$$\hat{t} = \sum_{\langle i,j \rangle, \sigma} (\hat{c}_{i\sigma}^\dagger \hat{c}_{j\sigma} + \hat{c}_{j\sigma}^\dagger \hat{c}_{i\sigma}), \quad \hat{U} = \sum_{j=1}^N \hat{n}_{j\uparrow} \hat{n}_{j\downarrow}. \quad (2)$$

In these expressions $\hat{c}_{i\sigma}$ are canonical Fermi operators which describe electrons on a two leg ladder, N represents the number of lattice sites in the ladder, $\langle i, j \rangle$ denotes nearest-neighbour sites, t is the hopping matrix element for the electrons, and U is the on-site Coulomb repulsion.

Below we present the exact ground states of the presented model for $N_p = 4$ particles and arbitrary ladder length, in the case of periodic boundary conditions and $u = U/t \geq 0$. The deduced ground state is a spin singlet state and from physical point of view describes the repulsive Hubbard interaction case ($U > 0$), for $t > 0$, or the attractive Hubbard interaction case ($U < 0$), for $t < 0$.

III. THE USED PROCEDURE

A. The construction of the basis wave vectors

The procedure we use is as follows. 1) First we number all lattice sites of the ladder as shown in Fig.1, taking into account periodic boundary conditions, and considering the number of rungs (e.g. $N/2$) integer number. 2) We identify the nine possible and qualitatively different microconfigurations in which four particles can be present into the ladder (see Fig.2). At this step we consider that the ladder legs are equivalent, and spin reversed microconfigurations are also equivalent. For the clarity of the mathematical notations we denote the possible microconfigurations by capital letters A to J , whose lower indices refer to the particle positions. In order to clearly distinguish the microconfigurations, we must consider in the C, E cases $i \neq j$, while in the F, J cases $j < k$ (see Fig.2). We further mention that in the process of defining a microconfiguration, at least one of the particles

is positioned at site number 1. Let us call these particles „starter” particles of the microconfiguration. For example, for the configuration A_i , the starter particles are two electrons with opposite spin; for the microconfiguration $F_{i,j,k}$ the starter particle is one electron with spin up, etc. (see Fig.2). 3) In the following step we define nine different type of orthogonal basis wave functions connected to each possible microconfiguration, and denoted with the same capital letter introduced in a ket-vector. For example, connected to the microconfiguration A_i , we have the basis wave vector $|A_i\rangle$; related to the microconfiguration B_i we have the basis wave vector $|B_i\rangle$, etc. 4) Since the lattice sites, legs, and spin orientations are equivalent, these properties must be reflected also at the level of the basis vectors. Because of this reason, each microconfiguration present in Fig.2 will be considered as generating microconfiguration and denoted by $O_{i,j,\dots}^{(1)}(n)$, where $n = 1, 2, \dots, 9$ denotes the microconfiguration number. For example $O_i^{(1)}(1) = A_i, O_i^{(1)}(2) = B_i, O_{i,j}^{(1)}(3) = C_{i,j}, \dots, O_{i,j,k}^{(1)}(9) = J_{i,j,k}$. 5) Now, connected to each generating microconfiguration $O_{i,j,\dots}^{(1)}(n)$, we define seven related („brother”) microconfigurations $O_{i,j,\dots}^{(m)}(n)$ (e.g. $m = 2, 3, \dots, 8$) by a) rotating the generating microconfiguration $m = 1$ by 180 degree along the longitudinal symmetry axis of the ladder, obtaining the $m = 2$ brother microconfiguration, b) rotating the generating microconfiguration $m = 1$ by 180 degree along the symmetry axis perpendicular to the ladder, obtaining the $m = 3$ brother configuration, c) rotating the $m = 3$ configuration by 180 degree along the longitudinal symmetry axis of the ladder, obtaining the $m = 4$ brother configuration, and finally d) reversing all spin orientations in the $m = 1, 2, 3, 4$ cases, we obtain the remaining $m = 5, 6, 7, 8$ brother microconfigurations. In this process it could happen that the starter particles situated at site 1 in the generating microconfiguration $m = 1$, arrive on the upper leg for a given brother configuration $m > 1$. An example of related („brother”) microconfigurations is presented in Fig.3. for the $|C_{i,j}\rangle$ case. 6) At the sixth step, the effective construction of the basis vectors follows. A given basis vector $|O_{i,j,\dots}^{(1)}(n)\rangle$, of type n (n being considered fixed), connected to the generating microconfiguration $O_{i,j,\dots}^{(1)}(n)$, is constructed as follows: a) The different brother microconfigurations $O_{i,j,\dots}^{(m)}(n)$ are all translated along the ladder such that the starter particles (see point 1)), arrive on each lattice site of the same leg. In this process, the translation must be such effectuated to not modify the interparticle positions and relative spin orientations inside the microconfiguration. b) After this step, all obtained microconfigurations are added. c) The expression is written in mathematical form by representing each microconfiguration by four creation operators acting on the bare

vacuum with no fermions present. In order to do this, we have to fix the order of creation operators for each basis vector type, which has been done as follows. For two doubly occupied sites, we write the creation operators of the couples next to each other, first the spin up, then the spin down contribution as $\hat{c}_{i\uparrow}^\dagger \hat{c}_{i\downarrow}^\dagger \hat{c}_{j\uparrow}^\dagger \hat{c}_{j\downarrow}^\dagger |0\rangle$. In the case of basis vectors containing one doubly occupied site at i we use $\hat{c}_{i\uparrow}^\dagger \hat{c}_{i\downarrow}^\dagger \hat{c}_{j\uparrow}^\dagger \hat{c}_{k\downarrow}^\dagger |0\rangle$. Finally, for basis vectors without doubly-occupied sites, the convention $\hat{c}_{i\uparrow}^\dagger \hat{c}_{j\uparrow}^\dagger \hat{c}_{k\downarrow}^\dagger \hat{c}_{l\downarrow}^\dagger |0\rangle$ is considered, where $i < j$, $k < l$ must hold.

For example, using the above described steps for the $|C_{i,j}\rangle$ basis wave vector, one finds the eight related („brother”) microconfigurations as shown in Fig.3. Furthermore, the mathematical expression of $|C_{i,j}\rangle$ taken for example at $i = 2, j = 4$, becomes

$$\begin{aligned}
|C_{2,4}\rangle = & \left((\hat{c}_{1\uparrow}^\dagger \hat{c}_{1\downarrow}^\dagger \hat{c}_{2\uparrow}^\dagger \hat{c}_{4\downarrow}^\dagger + \hat{c}_{2\uparrow}^\dagger \hat{c}_{2\downarrow}^\dagger \hat{c}_{3\uparrow}^\dagger \hat{c}_{5\downarrow}^\dagger + \dots) \right. \\
& + (\hat{c}_{(\frac{N}{2}+1)\uparrow}^\dagger \hat{c}_{(\frac{N}{2}+1)\downarrow}^\dagger \hat{c}_{(\frac{N}{2}+2)\uparrow}^\dagger \hat{c}_{(\frac{N}{2}+4)\downarrow}^\dagger + \hat{c}_{(\frac{N}{2}+2)\uparrow}^\dagger \hat{c}_{(\frac{N}{2}+2)\downarrow}^\dagger \hat{c}_{(\frac{N}{2}+3)\uparrow}^\dagger \hat{c}_{(\frac{N}{2}+5)\downarrow}^\dagger + \dots) \\
& + (\hat{c}_{4\uparrow}^\dagger \hat{c}_{4\downarrow}^\dagger \hat{c}_{3\uparrow}^\dagger \hat{c}_{1\downarrow}^\dagger + \hat{c}_{5\uparrow}^\dagger \hat{c}_{5\downarrow}^\dagger \hat{c}_{4\uparrow}^\dagger \hat{c}_{2\downarrow}^\dagger + \dots) \\
& + (\hat{c}_{(\frac{N}{2}+4)\uparrow}^\dagger \hat{c}_{(\frac{N}{2}+4)\downarrow}^\dagger \hat{c}_{(\frac{N}{2}+3)\uparrow}^\dagger \hat{c}_{(\frac{N}{2}+1)\downarrow}^\dagger + \hat{c}_{(\frac{N}{2}+5)\uparrow}^\dagger \hat{c}_{(\frac{N}{2}+5)\downarrow}^\dagger \hat{c}_{(\frac{N}{2}+4)\uparrow}^\dagger \hat{c}_{(\frac{N}{2}+2)\downarrow}^\dagger + \dots) \\
& \left. + \hat{c}_{1\uparrow}^\dagger \hat{c}_{1\downarrow}^\dagger \hat{c}_{4\uparrow}^\dagger \hat{c}_{2\downarrow}^\dagger + \hat{c}_{2\uparrow}^\dagger \hat{c}_{2\downarrow}^\dagger \hat{c}_{5\uparrow}^\dagger \hat{c}_{3\downarrow}^\dagger + \dots \right) |0\rangle. \tag{3}
\end{aligned}$$

We underline at this step, that because of the fixed conventions presented above, somethimes an additional negative sign arises in the process of writing the mathematical expressions corresponding to basis vector components shifted from the end to the beginning of the ladder in the presence of periodic boundary conditions. For example if we shift once more $\hat{c}_{1\uparrow}^\dagger \hat{c}_{N/2\uparrow}^\dagger \hat{c}_{2\downarrow}^\dagger \hat{c}_{3\downarrow}^\dagger |0\rangle$, according to the fixed conventions one obtains $\hat{c}_{2\uparrow}^\dagger \hat{c}_{1\uparrow}^\dagger \hat{c}_{3\downarrow}^\dagger \hat{c}_{4\downarrow}^\dagger |0\rangle = -\hat{c}_{1\uparrow}^\dagger \hat{c}_{2\uparrow}^\dagger \hat{c}_{3\downarrow}^\dagger \hat{c}_{4\downarrow}^\dagger |0\rangle$.

B. The deduction of the ground-state wave function

Our basic observation leading to the solution of the problem is that by applying the Hamiltonian \hat{H} to a basis wave function $|O_{i,j,\dots}^{(1)}(n_1)\rangle$ holding a fixed $n = n_1$, only contributions of the form $|O_{i,j,\dots}^{(1)}(n)\rangle$ with $n = 1, 2, \dots, 9$ can be obtained as a result. Consequently nine (e.g. $n = 1, 2, \dots, 9$) analytic equations building up a linear system of equations of the form

$$\hat{H}|O_{i,j,\dots}^{(1)}(n)\rangle = \sum_{n'=1}^9 \sum_{i',j',\dots} a_{i',j',\dots}^{n,n'} |O_{i',j',\dots}^{(1)}(n')\rangle, \tag{4}$$

provide the solution of the problem for arbitrary ladder length (e.g. arbitrary N), where $a_{i',j',\dots}^{n,n'}$ are numerical coefficients. For example, in the case of $n = 1$ (e.g. $|A_i\rangle = |O_i^{(1)}(1)\rangle$), Eq.(4) becomes

$$\hat{H}|A_i\rangle = 2u|A_i\rangle - |D_{i,i}\rangle - \Theta(i > 2)|C_{i-1,i}\rangle - \Theta(i \leq N/4)|C_{i,i+1}\rangle, \quad (5)$$

where $\Theta(K) = 1$ if the condition K is satisfied, otherwise $\Theta(K) = 0$, and we must have $1 < i \leq 1 + N/4$. Analogously, for $n = 2$ (e.g. $|B_i\rangle = |O_{i,j,\dots}^{(1)}(2)\rangle$), Eq.(4) gives

$$\hat{H}|B_i\rangle = 2u|B_i\rangle - \Theta(i > 1)|D_{i,i}\rangle - \Theta(i > 1)|E_{i-1,i}\rangle - \Theta(i \leq N/4)|E_{i,i+1}\rangle, \quad (6)$$

where for the index i one must have $1 \leq i \leq 1 + N/4$, and similar equations are obtained for the remaining $n = 3, 4, 5, \dots, 9$ index values as well. Consequently, the nine orthogonal basis vectors presented in Fig.2. provide nine analytic self-consistent linear equations (e.g. Eq.(4)), containing the ground state of the problem. This means that solving the secular equation related to Eq.(4) we arrive in a subspace of the original Hilbert space which contains the ground state. The ground state energy E_g is the minimum possible energy provided by the mentioned secular equation, and the ground state wave function is the eigenvector corresponding to E_g . The ground state energy and the ground state wave function must be numerically obtained from the system of equations Eq.(4). The ground state nature of the so obtained solution has been tested by numerical exact diagonalization taken on the full Hilbert space at different N values.

The leading terms for two ground state wave functions deduced at a fixed N and two different $u = U/t$ values are exemplified in the Appendix A.

The fact that the solution of the ground state of four particles in an arbitrary large two leg ladder can be exactly given in Eq.(4), is related to the observation that the possible n values (describing the different type of orthogonal basis vectors entering into the problem) are not changing if N is increased. Consequently, nine analytical equations will provide the solution in Eq.(4) independent of how large the N value is. But this does not mean that increasing N in the course of the numerical treatment of Eq.(4), the same number of equations provided by Eq.(4) are encountered. This is because even if the analytic expression of $\hat{H}|O_{i,j,\dots}^{(1)}(n)\rangle$ at a fixed n is the same for all N , the domains covered by the indices i, j, \dots in $|O_{i,j,\dots}^{(1)}(n)\rangle$ depend on the N value. For example, the Eq.(5) represents the unique analytic equation for the $|A_i\rangle$ base vector at arbitrary N . But during the numerical treatment of Eq.(5), all

equations for different i values must be considered. Since $i \leq 1 + N/4$ holds, the unique analytic equation (5), will provide an increasing number of different numerical equations by increasing N . But even in this case, the Hilbert space region defined by Eq.(4) containing the ground state, has an accentuatedly lower dimension d_{red} than the dimension d_H of the full Hilbert space of the problem. For example, at $N = 16$ we have $d_H = 14400$, $d_{red} = 287$, while at $N = 32$ one has $d_H = 2.410^5$, but $d_{red} = 2141$. As seen, at least two orders of magnitude reduction in the number of basis wave vectors is encountered in the treatment of the problem.

At the level of principle, Eq.(4), based on symmetry properties, delimitates the region of the Hilbert space where the ground state is placed. We must however emphasize that these symmetry properties, besides the symmetries of the system, depend on the microscopic parameters of the Hamiltonian as well. For example, Eq.(4) contains the ground state wave function only for $u > 0$.

IV. THE PROPERTIES OF THE GROUND STATE

Once the exact ground state wave function is known, the ground state itself can be characterized. Starting on this line, in this Section we exemplify the physical properties of the deduced ground state at $N = 28$.

A. Leading terms in the ground state, and ground state expectation values

We analyze first the u dependence of the leading terms of the ground state wave function $|\Psi_g\rangle$. As seen from Appendix A., at low u the main contributions in $|\Psi_g\rangle$ are obtained from relatively closely situated (e.g. almost nearest-neighbour) electrons with opposite spin („pairs”), the placement of the two pairs being such to maximize the interpair distance. Indeed, at $u = 3$, the leading terms in Appendix A. are the $|D_{7,7}\rangle, |E_{7,8}\rangle, |C_{7,8}\rangle, |D_{6,6}\rangle$ type of contributions, which as seen from Fig.2. (taking into account that the described system is a two leg ladder ring with 14 rungs), describe indeed this situation. As long as u is increased, the „pairs” in the leading terms tend to form double occupancies (as seen in Appendix. A. for $u = 100$), the distance between the pairs remaining considerably high.

Now we turn to analyze ground state expectation values. The ground state expectation

value of the kinetic energy term is presented in Fig.4. As seen, a non-monotonic behaviour is obtained. The general tendency for the decrease of the absolute value of E_{kin} in function of u at high u can be understood by the double occupancy formation. The physical reason for the presence of the maximum in E_{kin} for $u < 15$ is not yet properly understood. Probably the decrease in the increase rate of the double occupancy at a given site above $u = 5$ causes this behaviour (see Fig.5.).

The ground state expectation value of the double occupancy per site $D = \langle \hat{n}_{i,\uparrow} \hat{n}_{i,\downarrow} \rangle$ is presented in Fig.5. The general tendency present in this figure is that the increasing u value leads to the increase of D . This can be understood if we remember that for $t < 0$ the analyzed situation describes the attractive on-site interaction case, hence by increasing u we increase the number of double occupancies.

B. Pair correlation functions

Pair correlations are analyzed via the density-density correlation function

$$C_n(r) = \frac{1}{N} \sum_{i=1}^N (\langle \hat{n}_i \hat{n}_{i+r} \rangle - \langle \hat{n}_i \rangle \langle \hat{n}_{i+r} \rangle), \quad (7)$$

and spin-spin correlation function defined by

$$C_{S^z}(r) = \frac{1}{N} \sum_{i=1}^N (\langle \hat{S}_i^z \hat{S}_{i+r}^z \rangle - \langle \hat{S}_i^z \rangle \langle \hat{S}_{i+r}^z \rangle) = \frac{1}{2N} \sum_{i=1}^N (\langle \hat{n}_{i,\uparrow} \hat{n}_{(i+r),\uparrow} \rangle - \langle \hat{n}_{i,\uparrow} \hat{n}_{(i+r),\downarrow} \rangle), \quad (8)$$

where $\hat{n}_i = \hat{n}_{i,\uparrow} + \hat{n}_{i,\downarrow}$, $\hat{n}_{i,\sigma} = \hat{c}_{i\sigma}^\dagger \hat{c}_{i\sigma}$, $\hat{S}_i^z = (\hat{n}_{i,\uparrow} - \hat{n}_{i,\downarrow})/2$, r measures the inter-site distance in lattice constant units, and $\langle \dots \rangle$ has the meaning of the ground state expectation value.

The behaviour of the spin-spin correlation function is presented in Fig.6. As seen, compared to the non-interacting case, the spin-spin correlation decreases if u is increased. Concerning the distance dependence of $C_{S^z}(r)$ at a fixed u , we see that even the short-range correlations are strongly (presumably exponentially) decreasing, and the spin correlation length covers practically only nearest-neighbour sites.

The density-density correlations are exemplified in Fig.7. The presented curves have a specific structure which can be understood based on the analyzes of the leading terms of the ground state wave function presented at the beginning of this Section. As observed there, in the ground state, two „pairs” tend to be situated at highest possible distance each from other, providing the behaviour presented in Fig.7.

V. SUMMARY AND CONCLUSIONS

We have deduced the exact ground state for four electrons in an arbitrary large two-leg Hubbard ladder and have analyzed the physical properties of the ground state in function of microscopic parameters of the model. The procedure is based on the construction in \mathbf{r} -space of nine different type of orthogonal basis vectors which span the subspace of the Hilbert space containing the ground state. In order to do this, we start from the possible microconfigurations of the four particles within the system. This microconfigurations are then rotated, translated and spin-reversed in order to build up the basis vectors of the problem. A closed system of linear equations is obtained whose secular equation, by its minimum energy solution, provides the ground state energy and the ground state wave function of the model. The dimensionality of the subspace containing the ground state is substantially less than the dimension of the full Hilbert space. The deduced ground state wave functions have been used for the calculation of ground state expectation values and correlation functions in the process of the characterization of ground state properties.

Acknowledgments

This work was supported by the Hungarian Scientific Research Fund through contract OTKA-T-037212. The numerical calculations have been done at the Supercomputing Lab. of the Faculty of Natural Sciences, Univ. of Debrecen, supported by OTKA-M-041537.

APPENDIX A: EXPLICIT GROUND STATE WAVE FUNCTIONS.

We present below the leading terms of explicit ground state wave functions deduced for $N = 28$, at $u = 3$ and $u = 100$. The ground state $|\Psi_g\rangle$ is normalized to unity, and contains ortho-normalized basis vectors.

At $u = 3$ we obtain for the ground state wave function

$$\begin{aligned} |\Psi_g(u = 3.0)\rangle = & \\ & 0.177614|D_{7,7}\rangle + 0.170007|E_{7,8}\rangle + 0.170006|C_{7,8}\rangle + 0.15878|D_{6,6}\rangle \\ & + 0.158091|C_{6,7}\rangle + 0.158089|E_{6,7}\rangle + 0.138593|D_{8,7}\rangle + 0.138593|D_{7,8}\rangle \\ & + 0.135254|C_{5,6}\rangle + 0.135236|E_{5,6}\rangle + 0.129199|D_{5,5}\rangle + 0.128869|D_{6,7}\rangle \end{aligned}$$

$$\begin{aligned}
& +0.128868|D_{7,6}\rangle + 0.110223|D_{5,6}\rangle + 0.110212|D_{6,5}\rangle + 0.103555|C_{4,5}\rangle \\
& +0.103502|E_{4,5}\rangle + 0.100914|G_{7,8,1}\rangle - 0.100914|G_{8,2,8}\rangle + 0.0974412|E_{6,8}\rangle \\
& +0.0974383|C_{6,8}\rangle - 0.0938371|G_{7,2,7}\rangle + 0.0938365|G_{6,7,1}\rangle + 0.093035|D_{7,9}\rangle \\
& +0.0917791|D_{4,4}\rangle + 0.0897459|D_{8,6}\rangle + 0.089745|D_{6,8}\rangle + 0.0870033|C_{5,7}\rangle \\
& +0.0869974|E_{5,7}\rangle + 0.0843159|D_{4,5}\rangle + 0.0842604|D_{5,4}\rangle - 0.0822647|J_{7,1,8}\rangle \\
& +0.082264|H_{7,7,14}\rangle - 0.0802686|G_{6,2,6}\rangle + 0.0802625|G_{5,6,1}\rangle + 0.080119|D_{5,7}\rangle \\
& +0.0801123|D_{7,5}\rangle + 0.0774351|G_{7,8,14}\rangle - 0.0771843|G_{8,2,9}\rangle + 0.0764892|H_{6,6,14}\rangle \\
& -0.0764889|J_{6,1,7}\rangle + 0.0746979|G_{6,7,14}\rangle - 0.0746978|G_{8,2,7}\rangle + 0.0744824|G_{7,8,2}\rangle \\
& -0.0744821|G_{7,2,8}\rangle + 0.0704993|C_{4,6}\rangle + 0.070455|E_{4,6}\rangle + 0.0666869|G_{5,6,14}\rangle \\
& -0.0666861|G_{7,2,6}\rangle - 0.0666109|G_{6,2,7}\rangle + 0.0666052|G_{6,7,2}\rangle + 0.0663597|C_{3,4}\rangle \\
& +0.0663115|E_{3,4}\rangle + 0.0654117|H_{5,5,14}\rangle - 0.0654063|J_{5,1,6}\rangle + 0.0650782|D_{8,8}\rangle \\
& +0.064882|D_{4,6}\rangle + 0.0648305|D_{6,4}\rangle - 0.0614256|G_{5,2,5}\rangle + 0.0613938|G_{4,5,1}\rangle \\
& +0.0599305|G_{7,9,1}\rangle + 0.0594696|E_{6,9}\rangle + 0.0594586|C_{6,9}\rangle + 0.0578123|G_{6,8,1}\rangle \\
& -0.0578118|G_{8,3,8}\rangle + 0.0574775|D_{7,10}\rangle + 0.0574745|D_{6,9}\rangle - 0.0555399|H_{6,13,7}\rangle \\
& +\dots
\end{aligned} \tag{A1}$$

while for $u = 100$ one has

$$\begin{aligned}
& |\Psi_g(u = 100)\rangle = \\
& 0.38466|B_7\rangle + 0.384611|A_7\rangle + 0.354728|B_6\rangle + 0.354558|A_6\rangle \\
& +0.306686|B_5\rangle + 0.306065|A_5\rangle + 0.243462|B_4\rangle + 0.241179|A_4\rangle \\
& +0.169981|B_3\rangle + 0.161576|A_3\rangle + 0.13959|B_8\rangle + 0.139581|A_8\rangle \\
& +0.0961638|B_2\rangle + 0.0652468|A_2\rangle + 0.0623588|E_{7,8}\rangle + 0.0623528|C_{7,8}\rangle \\
& +0.0615656|D_{7,7}\rangle + 0.0591513|E_{6,7}\rangle + 0.0591339|C_{6,7}\rangle + 0.0567649|D_{6,6}\rangle \\
& +0.0529133|E_{5,6}\rangle + 0.0528502|C_{5,6}\rangle + 0.0490391|D_{5,5}\rangle + 0.044012|E_{4,5}\rangle \\
& +0.0437798|C_{4,5}\rangle + 0.0387863|D_{4,4}\rangle + 0.0330753|E_{3,4}\rangle + 0.0322208|C_{3,4}\rangle \\
& +0.0265348|D_{3,3}\rangle + 0.0223424|D_{8,8}\rangle + 0.0212907|E_{2,3}\rangle + 0.018145|C_{2,3}\rangle \\
& +0.0171881|B_1\rangle + 0.0129086|D_{2,2}\rangle + 0.011569|E_{1,2}\rangle + 0.00249322|D_{8,7}\rangle \\
& +0.00249322|D_{7,8}\rangle + 0.00236474|D_{6,7}\rangle + 0.00236474|D_{7,6}\rangle + 0.00211441|D_{5,6}\rangle \\
& +0.00211441|D_{6,5}\rangle + 0.00175512|D_{4,5}\rangle + 0.00175512|D_{5,4}\rangle + 0.00130539|D_{3,4}\rangle
\end{aligned}$$

$$\begin{aligned}
&+0.00130539|D_{4,3}\rangle - 0.0012476|G_{8,2,8}\rangle + 0.0012476|G_{7,8,1}\rangle + 0.00121559|E_{6,8}\rangle \\
&+0.00121536|C_{6,8}\rangle + 0.00118331|G_{6,7,1}\rangle - 0.00118331|G_{7,2,7}\rangle + 0.0011211|E_{5,7}\rangle \\
&+0.00112029|C_{5,7}\rangle - 0.00105805|G_{6,2,6}\rangle + 0.00105805|G_{5,6,1}\rangle + 0.000969643|E_{4,6}\rangle \\
&+0.000966692|C_{4,6}\rangle - 0.000878259|G_{5,2,5}\rangle + 0.000878259|G_{4,5,1}\rangle + 0.000788073|D_{2,3}\rangle \\
&+0.00078803|D_{3,2}\rangle + 0.000771179|E_{3,5}\rangle + 0.000760318|C_{3,5}\rangle - 0.000653214|G_{4,2,4}\rangle \\
&+ \dots
\end{aligned} \tag{A2}$$

-
- AMAYA-TAPIA, A., GASANEO, G., OVCHINIKOV, S., MACEK, S., LARSEN, S., Y., 2004, Jour. Math. Phys. **45**, 3533.
- BOWEN, G., GULÁCSI, M., 2001, Phil. Mag. **B81**, 1409.
- CHAN, R., GULÁCSI, M., 2002, Phil. Mag. Lett. **81**, 673, (2001); *ibid.* **82**, 671.
- CHEN, G., H., WU, Y., S., 2002, Phys. Rev. **B66**, 155111.
- DAVYDYCHEV, A., I., DELBOURGO, R., 2004, Jour. of Phys. **A37**, 4871.
- GOLDEN, J., M., HALPERIN, B., I., 2002, Phys. Rev. **B65**, 115326.
- GULÁCSI, M., 1997, Phil. Mag. **B76**, 731.
- GULÁCSI, M., BEDELL, K., S., 1994, Phys. Rev. Lett. **72**, 2765.
- GULÁCSI, M., ANDERSON, P., W., 1998, Jour. Magn. Magn. Matter. **177**, 319.
- GULÁCSI, ZS., 2004a, Phil. Mag. Lett. **84**, 405.
- GULÁCSI, ZS., 2004b, Phys. Rev. **B69**, 054204.
- GULÁCSI, ZS., VOLLHARDT, D., 2003, Phys. Rev. Lett. **91**, 186401.
- HALFPAP, O., 2001, Annalen Der Physik **10**, 623.
- HONNER, G., GULÁCSI, M., 1977, Z. Phys. **B104**, 733.
- HONNER, G., GULÁCSI, M., 1997, Phys. Rev. Lett. **78**, 2180.
- HONNER, G., GULÁCSI, M., 1998, Jour. Magn. Magn. Matter. **184**, 307; 1998, Phys. Rev. **B58**, 2662; 1999, Jour. Supercond. **12**, 237.
- KOCHERESHKO, V., P., et al., 2003, Physica **E17**, 197.
- KOVÁCS, E., GULÁCSI, ZS., 2001, Phil. Mag. **B81**, 1557.
- KOVÁCS, E., GULÁCSI, ZS., 2004, same issue.
- MAKSYM., P., A., IMAMURA, H., MALLON, G., P., and AOKI, H., 2000, Jour. of Phys. **C12**,

R299.

MCCULLOCH, I., P., GULÁCSI, M., 2002, Europhys. Lett. **57**, 852.

MCCULLOCH, I., P., JOUZAPAVICIUS, I., P., ROSENGREN, A., GULÁCSI, M., 2001, Phil. Mag. Lett. **81**, 869; 2002 Phys. Rev. **B65**, 52410.

OKABE, T., YAMADA, H., 2004, Modern Phys. Lett. **B18**, 269.

ORIGNAC, E., CITRO, R., 2003, Eur. Phys. Jour. **B33**, 419.

ORIGNAC, E., POIBLANC, D., 2003, Phys. Rev. **B68**, 052504.

PAPADOPOULOS, C., G., 2001, Comp. Phys. Commun. **137**, 247.

SACKETT, C., A., 2000, Nature **404**, 256.

SENTHIL, T., 2004, 10 Nov., cond-mat/0411275.

SHANKAR, R., 1994, Rev. Mod. Phys. **66**, 129.

SIGRIST, M., TSUNETSUGU, H., UEDA, K., 1991, Phys. Rev. Lett. **67**, 2211.

TOMONAGA, S., 1950, Progr. Theor. Phys. Osaka **5**, 544.

TORRES, J., 2002, Ann. Phys. Paris, **27**, 1.

TRAYNOR, C., A., ANDERSON, J., B., BOGHOSIAN, B., M., 1991, Jour. Chem. Phys. **94**, 3657.

UESAKA, Y., NAKATANI, Y., HAYASHI, N., 1993, Jour. Magn. Magn. Matter. **123**, 209.

ZHANG, N., G., HENLEY, C., L., 2004, Eur. Phys. Jour. **B38**, 409.

ZHOU, X., R., GUO, L., MENG, J., ZHAO, E., G., 2002, Commun. in Theor. Phys. **37**, 583.

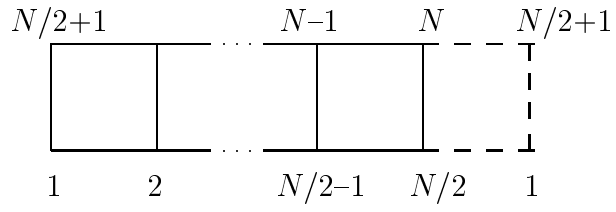


FIG. 1: The numbering of the lattice sites for the two leg ladder taken with periodic boundary conditions. N is considered even.

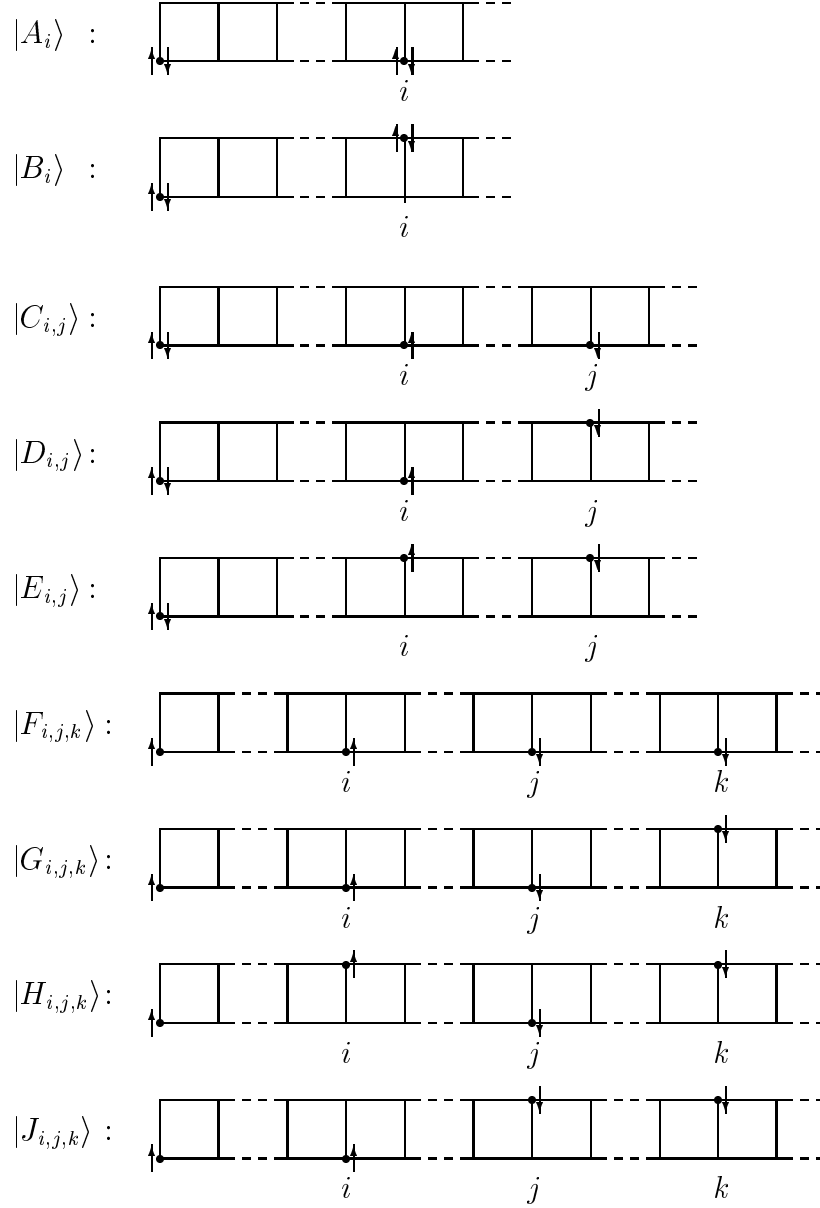


FIG. 2: The different possible types of basis vectors. We note that for the cases C, E $i \neq j$, while for F, J $j < k$ is considered, respectively. In the cases F, G, H, J , the double occupancy is forbidden.

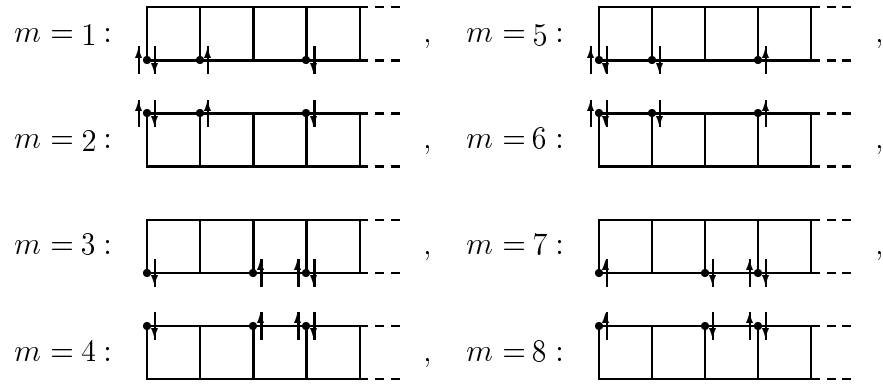


FIG. 3: The brother microconfigurations together with their m index for the $|C_{i,j}\rangle$ basis wave vector.

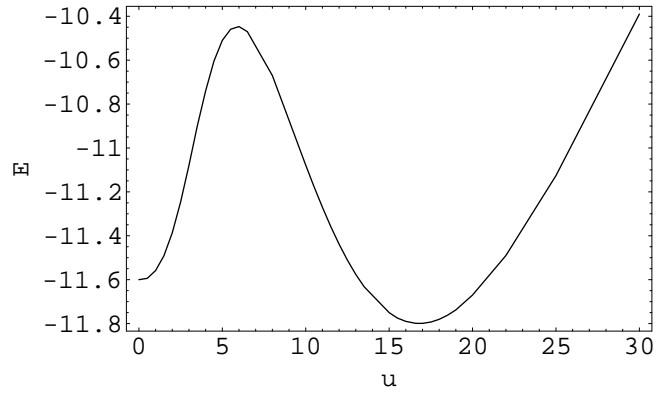


FIG. 4: The dependence of the kinetic energy on u .

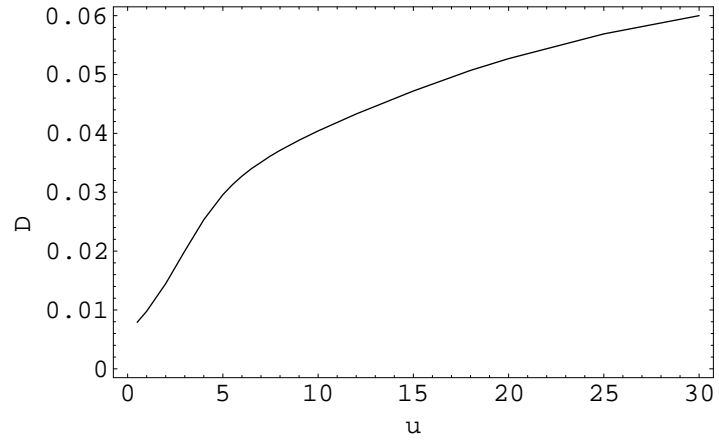


FIG. 5: The dependence of the double occupancy per site $D = \left| \frac{E_{pot}}{uN} \right|$ on u .

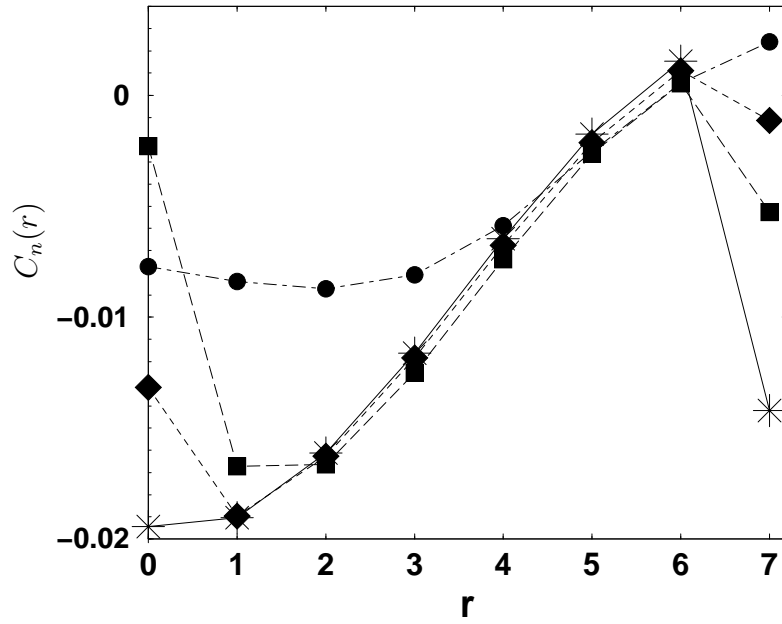


FIG. 6: The density-density correlation function for $u = 0$ (dots, dot-dashed line), $u = 10$ (squares, long dashed line), $u = 30$ (diamonds, short dashed line), $u = 100$ (stars, continuous line). r is the distance in lattice constant units

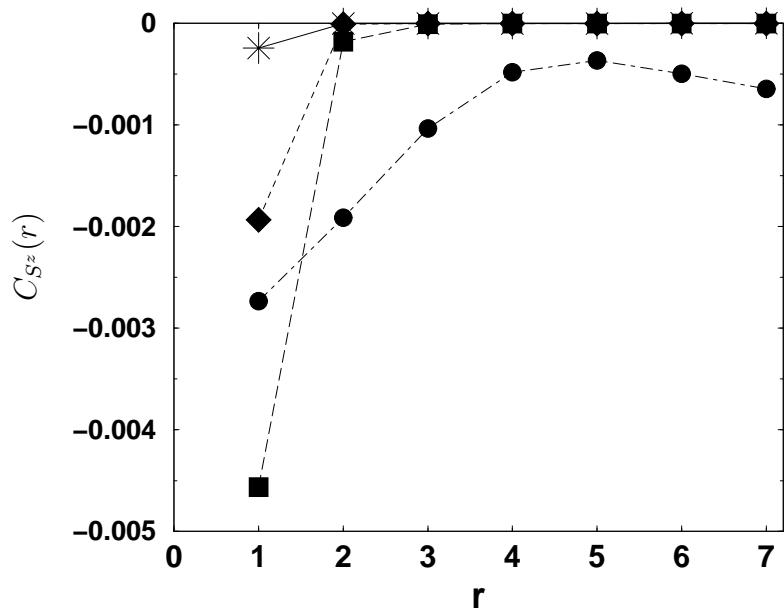


FIG. 7: The \hat{S}^z - \hat{S}^z correlation function for $u = 0$ (dots, dot-dashed line), $u = 10$ (squares, long dashed line), $u = 30$ (diamonds, short dashed line), $u = 100$ (stars, continuous line). r is the distance in lattice constant units